Restoration of magnetization reversal under hydrostatic pressure in the lightly electron-doped manganite compound (Ca,Sr)$Mn_{0.95}Sb_{0.05}O_3$

Takahiro Fujiwara,[1] Michiaki Matsukawa,[1,*] Takahiro Aoyagi,[1] Satoru Kobayashi,[1] Shigeki Nimori,[2] and Ramanathan Suryanarayanan[3]

[1]*Department of Materials Science and Engineering, Iwate University, Morioka 020-8551, Japan*
[2]*National Institute for Materials Science, Tsukuba 305-0047,Japan*
[3]*Laboratoire de Physico-Chimie de L'état Solide, CNRS, UMR8182, Université Paris-Sud, 91405 Orsay,France*

(Dated: June 24, 2021)

We report on the anomalous magnetization reversal under hydrostatic pressure in the lightly electron-doped manganite compound $(Ca_{1-x}Sr_x)Mn_{0.95}Sb_{0.05}O_3$ with its fixed carrier content. In a weakly magnetic field cooled measurement, diamagnetic magnetization is observed for $x \leq 15\%$, which changes to positive values for $x > 15\%$. However, on an application of pressure on the samples with $x = 16\%$ and 17%, magnetization reverses sign and diamagnetism is restored. We present a magnetic phase diagram as a function of Sr concentration, under both ambient and hydrostatic pressures. To understand better the thermodynamical properties of this system, we have measured the specific heat as a function of temperature under a field cooling of 100 Oe. Our data show no anomalies associated with the temperature dependent magnetization reversal, indicating the absence of a long-rang magnetic ordering. The *ac* magnetic susceptibility measurement points to the existence of magnetic frustration for the Sr substituted samples exhibiting diamagnetic behavior.

PACS numbers: 75.50.-y,75.47.Gk,62.50.-p,72.20.Pa

Extensive studies on the magnetization reversal or negative magnetization in magnetic materials demonstrate the potential use in magnetic memory and related applications. $CaMnO_3$, the end member of the $Ca_{1-x}La_xMnO_3$ system, undergoes a G-type antiferromagnetic transition around $T_N \sim 120$ K, accompanied by a weak ferromagnetic component,[1] where each spin of the Mn ions is antiparallel to the nearest neighbors of Mn. In recent years, the electron-doped manganite system $(x < 0.5)$[2] has attracted much attentions because of the possibility of observing a negative magnetoresistance effect similar to that observed in its counterparts, in the so-called hole-doped manganites, for $x > 0.5$. The negative magnetization phenomena in manganites were originally reported in compounds with two sublattices of Mn ions and rare-earth ions (Nd, Gd, Dy)[3–5] Some of these studies were discussed on the basis of a ferrimagnetic scenario leading to a negative magnetization at temperatures below a compensation temperature, where Mn and some rare-earths sublattices are antiferrmagnetically coupled. Earlier, a negative magnetization in $CaMnO_3$ with B-site substitution had been reported[6]. Recently, we demonstrated the effect of the hydrostatic pressure on magnetic and transport properties in the lightly electron-doped manganite $CaMn_{1-x}Sb_xO_3$[7]. Anomalous magnetization reversals were clearly observed for x=0.05 and 0.08 in the field-cooled magnetization while the application of external pressure induced a suppression of the negative magnetization. A theoretical work on lightly electron-doped manganite $CaMnO_3$ predicted that spin canting in the G-type antiferromagnetic structure is realized by electron doping through the double exchange mechanism.[8,9] The weak FM component observed in the Ce-substituted $CaMnO_3$ is well explained by the spin-canting G-type AFM state with the double-exchange hopping of electrons. For the lightly electron-doped samples with $CaMn_{1-x}Sb_xO_3$, we believe that a weak ferromagnetic trend in their MT curves is compatible with the present canted AFM scenario. The larger Sb substitution at the Mn site introduces the local lattice distortion of $Mn^{3+}O_6$ associated with e_g-electron doping and then changes the orbital state of e_g-electron through the local John-Teller effect. As a result, it gives rise to a considerable variation in local spin configuration existing at the nearest neighbor of its Sb ion, leading to the formation of diamagnetic clusters within its matrix. The canted AFM matrix stablized by light electron doping contributes to a weak ferromagnetic component. On the other hand, the diamagnetic clusters are simultaneously formed through the local lattice deformation due to the substitution of Sb with its larger ionic radius. In this paper, we report the magnetization reversal under hydrostatic pressure in the lightly electron-doped manganite compound $(Ca_{1-x}Sr_x)Mn_{0.95}Sb_{0.05}O_3$ with its fixed carrier content. Furthermore, to understand better the thermodynamical properties of the present system, we carry out the specific heat measurement for these compounds over a wide range of temperature.

Polycrystalline samples of $(Ca_{1-x}Sr_x)Mn_{0.95}Sb_{0.05}O_3$ (x=0.0, 0.05, 0.10, 0.15, 0.16, 0.17, and 0.2) were prepared by using a solid-state reaction method. The stoichiometric mixtures of high purity $CaCO_3$, Mn_3O_4, Sb_2O_3 and $SrCO_3$ powders were calcined in air at 1000°C for 24 h. The products were then ground and pressed into cylindrical pellets. The pellets were finally sintered at 1400 $\sim$ 1450°C for 12 h. X-ray diffraction data obtained by using Rigaku Ultima IV revealed that all samples had almost a single phase with an orthorhombic structure ($Pnma$)[10]. The lattice parameters and unit-cell volume estimated from X-ray diffraction patterns using RIETAN-FP program are shown as a function of Sr content in Fig. 1, We note the linear relationship between the volume and the Sr substitution at the Ca site in present system, as previously reported in $(Gd_{0.08}Ca_{1-x}Sr_x)MnO_3$.[11] X-ray photoemission spectroscopy on the $CaMn_{0.8}Sb_{0.2}O_3$ sample performed at room temperature strongly support that the valence of the Sb ion is 5+ .[12] The electron probe micro analyzer (EPMA) analysis on the nominal samples with x=0.0, 0.15, 0.16, and 0.17 is listed in Table I. We note that our samples prepared by the solid state reaction method are close to the nominal composition and there is a quite small difference in the Mn content between each sample. The dc magnetization measurement was carried out using the commercial superconducting quantum interference device (SQUID) magnetometers at Iwate University and at the National Institute for Materials Science (NIMS). The ac magnetic susceptibility measurement was measured as a function of temperature for frequencies ranging from 1 Hz to 1000 Hz under the ac magnetic field of 5 Oe at NIMS. The specific heat measurement in field cooled mode was carried out from 120 K down to 2 K using the physical property measuring system (Quantum Design PPMS).

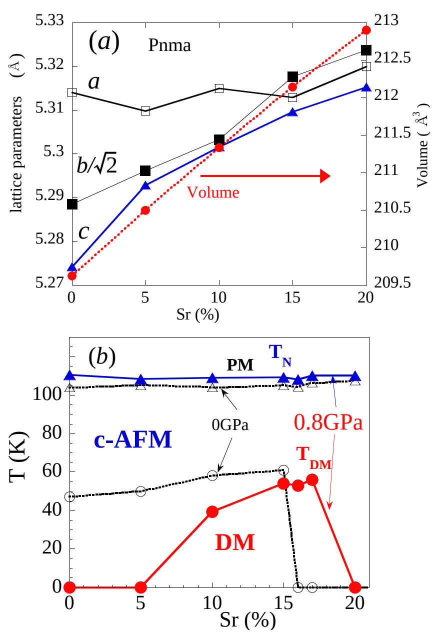

Fig. 1: (Color online) (a)The lattice parameters and unit-cell volume as a function of Sr estimated from X-ray diffraction patterns of $(Ca_{1-x}Sr_x)Mn_{0.95}Sb_{0.05}O_3$. The unit-cell volume is nearly proportional to an increase of the Sr content. (b) The magnetic phase diagram of the Sr-substituted $(Ca_{1-x}Sr_x)Mn_{0.95}Sb_{0.05}O_3$, where PM, c-AFM, and DM denote paramagnetic, canted antiferromagnetic, and diamagnetic phases, respectively. T_{DM} and T_N represent the diamagnetic and canted antiferromagnetic transition temperatures.

TABLE I: EPMA analysis of $(Ca_{1-x}Sr_x)Mn_{0.95}Sb_{0.05}O_3$ (x=0.0, 0.15, 0.16, and 0.17) .

Element nominal composition	Ca	Sr	Mn	Sb	O
$CaMn_{0.95}Sb_{0.05}O_3$	1.010	0.00	0.943	0.048	3.02
$(Ca_{0.85}Sr_{0.15})Mn_{0.95}Sb_{0.05}O_3$	0.845	0.164	0.927	0.048	3.03
$(Ca_{0.84}Sr_{0.16})Mn_{0.95}Sb_{0.05}O_3$	0.836	0.177	0.925	0.048	3.02
$(Ca_{0.83}Sr_{0.17})Mn_{0.95}Sb_{0.05}O_3$	0.830	0.187	0.918	0.047	3.04

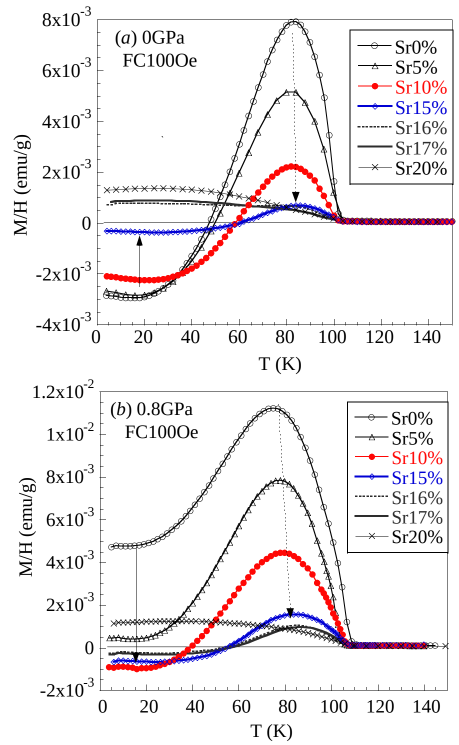

Fig. 2: (Color online) Temperature dependence of the field-cooled magnetic susceptibility M/H for $(Ca_{1-x}Sr_x)Mn_{0.95}Sb_{0.05}O_3$ recorded under both ambient and hydrostatic pressures, (a) and (b).

Now, let us show in Fig.2 , the effect of Sr substitution at Ca site on the temperature dependent magnetization reversal for $(Ca_{1-x}Sr_x)Mn_{0.95}Sb_{0.05}O_3$. For the parent sample, upon lowering temperature the magnetization shows a large enhancement near 80 K and then the diamagnetic behavior is observed at lower temperatures. The Sr substitution at Ca site affects a strong suppression in the magnetic peak located around 80 K from 8×10^{-3} emu/g at x=0.0 through 5×10^{-3} emu/g at x=0.05 down to 2×10^{-3} emu/g at x=0.10. On the other hand, a negative value of the magnetization at 20 K is not largely changed in the case of Sr content up to x=0.10. The effect of Sr substitution on the crystal structures of perovskite manganites $(Ca_{1-x}Sr_x)MnO_3$ and $(Gd_{0.08}Ca_{1-x}Sr_x)MnO_3$ brings a suppression of the Mn-O-Mn buckling.[11,13] It is pointed out in lightly electron doped manganites[11] that the unit-cell volume in-

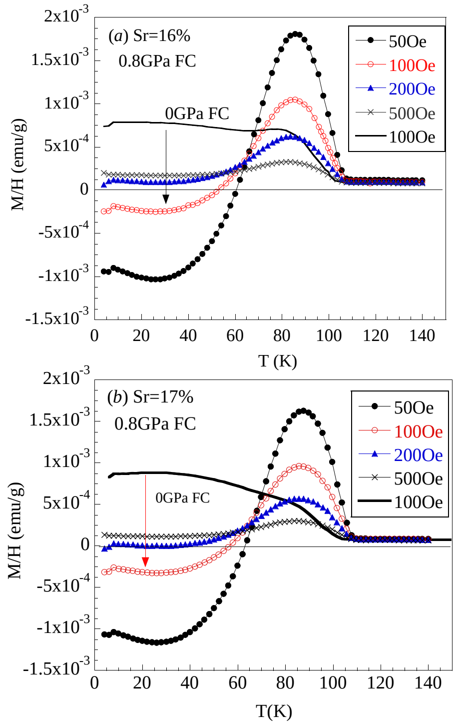

Fig. 3: (Color online) Temperature dependence of the field-cooled magnetic susceptibility M/H for $(Ca_{1-x}Sr_x)Mn_{0.95}Sb_{0.05}O_3$ recorded under a hydrostatic pressure of 0.8 GPa. (a) x=0.16, and (b) x= 0.17. For comparison, the solid curves represent the FC data without the applied pressure.

creases linearly with an increase of the Sr substitution at the Ca site, which is caused by not the expansion of Mn-O bond length but a suppression of the tilting of the MnO_6 octahedra. Our lattice data also exhibit the linear relationship between the volume and Sr content as shown in Fig.1 (a). In the case of low Sr, the Sr ions are distributed within the canted AFM matrix contributing to weak ferromagnetic component. If the Sr substitution at Ca site gives rise to a suppression of the buckling of Mn-O-Mn bonds, it then results in a suppression of the magnetic peak. A further increase of Sr ions above 10% affects diamagnetic clusters occupying small regions around Sb site and at last the addition of Sr beyond 15% suppresses the diamagnetic magnetization . We expect that the tilting of $Mn^{3+}O_6$ octahedron near Sb ion is relaxed by the higher Sr substitution, giving a decrease in the negative component. It is an interesting feature that the disappearance of the negative magnetization accompanies a collapse of the clear peak in the magnetization curve.

Next, we show in Fig.2 (b) the magnetization curve under the applied pressure of 0.8 GPa, to examine further the lattice effect on the magnetic properties of $(Ca_{1-x}Sr_x)Mn_{0.95}Sb_{0.05}O_3$. Application of the hydrostatic pressure on the parent sample enhances the mag-

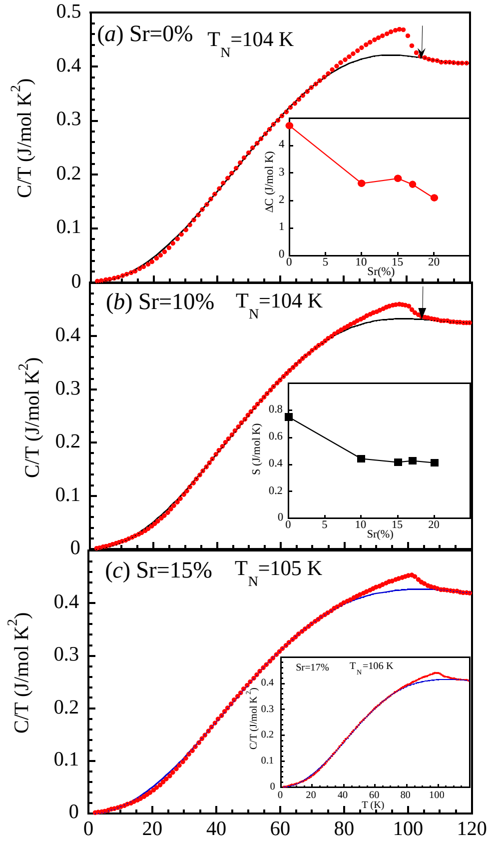

Fig. 4: (Color online) C/T vs T for $(Ca_{1-x}Sr_x)Mn_{0.95}Sb_{0.05}O_3$ measured in field cooling of 100 Oe . (a) x=0, (b)x=0.1 and (c)x=0.15 (the inset of (c) x=0.17). The solid curves denote the lattice contribution estimated from a polynomial approximation. The insets of (a) and (b) represent the magnetic heat jump ΔC and the magnetic entropy S_{mag} associated with the magnetic transition, respectively.

netic susceptibility over a wide range of temperatures, the magnitude of M/H at 80 K increases from 8×10^{-3} emu/g at 0 GPa to 1.1×10^{-2} emu/g at 0.8 GPa, and the diamagnetic behavior at lower temperatures is not visible. Upon increasing Sr content up to 15%, the magnetic peak is considerably suppressed as observed in the case of ambient pressure. However, the low temperature magnetization curve recorded at 0.8 GPa is changed from positive values at Sr=0% and 5% to negative values at Sr=10%. There exist qualitative differences in the Sr dependence of the low-T magnetization between both ambient and hydrostatic pressures. These findings are close to differences in the response of the lattice between the chemical and physical pressure effects. In previous works on the effect of pressure on the atomic structure of manganites, below 2 GPa all three Mn-O bond lengths are compressed but the Mn-O bond angles show no obvious changes.[14,15] According to these studies, the applied pressure on present samples causes a shrinkage

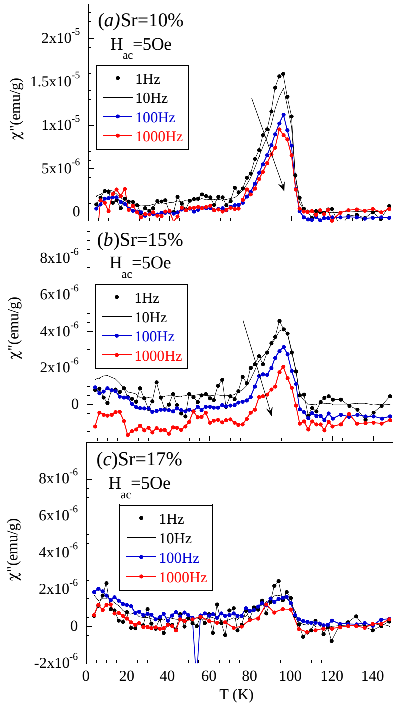

Fig. 5: (Color online) The imaginary parts of *ac* magnetic susceptibility of $(Ca_{1-x}Sr_x)Mn_{0.95}Sb_{0.05}O_3$ as a function of temperature collected at zero *dc* magnetic field for frequencies ranging from 1 Hz to 1000 Hz. (a) $x = 0.10$, (b) $x = 0.15$, and (c) $x = 0.17$. The amplitude of the *ac* magnetic field H_{ac} was 5 Oe. The arrows point to the direction of increasing frequencies.

of Mn-O bond lengths, resulting in the enhancement of the magnetic coupling between Mn ions, which explains well both the steep increase of M/H and a stable rise of the weak ferromagnetic transition temperature. For the samples with $x = 16\%$ and 17%, the diamagnetism reappears under 0.8 GPa in spite of no indication of the negative magnetization under the ambient pressure, as shown in Fig. 3 . The local JT distortion is more enhanced through the orbital lattice coupling under the applied pressure in comparison to the pressure induced enhancement of magnetic interaction, which is probably close to the reappearance of canted spin clusters contributing to a diamagnetism. The magnetic phase diagram of $(Ca_{1-x}Sr_x)Mn_{0.95}Sb_{0.05}O_3$ established at 100 Oe under the ambient and hydrostatic pressures is summarized in the inset of Fig.1 (b).

To understand further the thermodynamical properties of this system, we performed the specific heat measurements over a wide range of temperatures under a field cooling of 100 Oe. Figure 4 shows the specific heat as a function of temperature from 2 K to 120 K for $(Ca_{1-x}Sr_x)Mn_{0.95}Sb_{0.05}O_3$ (x=0, 0.1, 0.15, and 0.17) . Here, the lattice contribution C_l is roughly estimated from a polynomial approximation as previously reported in manganites.[16] ΔC represents the maximum value of the magnetic contribution $C - C_l$ and the magnetic entropy is estimated by integrating $(C - C_l)/T$ with respect to T. We observe clear anomalies associated with a magnetic transition near T_N but no visible changes in the specific heat data at temperatures where the diamagnetic behaviors appear. Our thermodynamical data strongly support that the temperature dependent magnetization reversal accompanies no long-rang magnetic ordering. It is expected from theses findings that short-range magnetic clusters around Sb ions have a close relationship with the appearance of observed weak diamagnetism. For the Sr substituted samples, both the magnetic heat jump and magnetic entropy are not largely changed. In particular, we do not find out distinct differences in the thermodynamical properties between the diamagnetic Sr15% sample and the weakly ferromagnetic Sr17% one.

Finally, we carried out the *ac* magnetic susceptibility measurements for $(Ca_{1-x}Sr_x)Mn_{0.95}Sb_{0.05}O_3$ (x 0.1, 0.15, and 0.17), in order to clarify the dynamical effect on the diamagnetic state. The temperature dependence of the imaginary parts, χ'', are registered at zero *dc* magnetic field with increasing frequency f ranging from 1 Hz to 1000 Hz , as shown in Figs. 5. For the parent Sr0% sample, a sharp peak in χ'' is observed around 100 K, which is good agreement with the *dc* magnetic measurement.[7] Upon increasing f, a second peak of χ' and χ'' located at 90 K slightly shifts towards lower temperatures. For lower Sr doping up to 10%, the amplitude of χ'' shows its strong decay with increasing frequency. When the Sr content exceeds 15%, the frequency dependence of *ac* magnetic susceptibility almost disappears. The frequency dependence of the *ac* magnetization indicates the signature of a spin-glass like character, but a substantial decrease of the peak in χ'' with increasing f is in contrast to the behavior of conventional spin-glass system[17], as previously pointed out in the phase-separated $Pr_{0.7}Ca_{0.3}MnO_3$.[18] The *ac* magnetic susceptibility measurement of the lower Sr substituted samples suggests the existence of magnetic frustration between diamagnetic clusters and canted antiferromagnetic matrix. In summary, we have demonstrated the remarkable influence of pressure on the magnetic properties of the title compound. For $x > 15\%$, the disappeared diamagnetic signal, reappears when the pressure is applied. However, the specific heat measurements do not reveal any magnetic phase transition. The *ac* susceptibility data indicate the existence of magnetic frustration.

* Electronic address: matsukawa@iwate-u.ac.jp

[1] J. B. MacChesney, H. J. Williams, J. F. Potter and R. C.

Sherwood, Phys. Rev. **164**, 779 (1967).

[2] H. Chiba, M. Kikuchi, K. Kasuba, Y. Muraoka and Y. Syono, Solid State Commun. **99**, 499 (1996).

[3] F. Bartolome, J. Herrero-Albillos, L. M. Garcia, J. Bartolome, N. Jaouen and A. Rogalev, J. Appl. Phys. **97**, 10A503 (2005).

[4] O. Pena, M. Bahout, K. Ghanimi, P. Duran, D. Gutierrez and C. Moure, J. Mater. Chem. **12**, 2480 (2002)

[5] C. A. Nordman, V. S. Achutharaman, V. A. Vasko, P. A. Kraus, A. R. Ruosi, A. M. Kadin and A. M. Goldman, Phys. Rev. B**54**, 9023 (1996).

[6] R. Ang, Y. P. Sun, Y. Q. Ma, B. C. Zhao, X. B. Zhu and W. H. Song, J. Appl. Phys. **100**, 063902 (2006).

[7] Y. Murano, M. Matsukawa, S. Ohuchi, S. Kobayashi, S. Nimori, R. Suryanarayanan, K. Koyama and N. Kobayashi, Phys. Rev. B**83**, 054437 (2011).

[8] C. Zener, Phys. Rev. 82, 403 (1951); P. G. deGennes, *ibid.* 118, 141 (1960).

[9] H. Ohnishi, T. Kosugi, T. Miyake, S. Ishibashi, and K. Terakura, Phys. Rev. B**85**, 165128 (2001).

[10] V. Poltavets, K. Vidyasagar and M.Jansen, J. Solid State Chem. **177**, 1285 (2004).

[11] S. Hirano, J. Sugiyama, T. Noritake, and T. Tani, Phys. Rev. B**70**, 094419 (2004).

[12] T. Fujiwara, M. Matsukawa, S. Ohuch, S.Kobayashi, R. Suryanarayanan, S. Nimori, J. Kor.Phys. Soc.62(2013) 1925.

[13] O. Chmaissem, B. Dabrowski, S. Kolesnik, J. Mais, D. E. Brown, R. Kruk, P. Prior, B. Pyles and J. D. Jorgensen, Phys. Rev. B**64**, 134412 (2001).

[14] C. Cui, T. A. Tyson, Z. Zhong, J. P. Carlo, and Y. Qin, Phys. Rev. B**67**, 104107 (2003).

[15] Z. Chen, T. A. Tyson, K. H. Ahn, Z. Zhong, and J. Hu, J. Magn. Magn. Mater. **322**, 3049(2010).

[16] J. E. Gordon, R. A. Fisher, Y. X. Jia, N. E. Phillips, S. F. Peklis, D. A. Wright and A. Zettl, J. Magn. Magn. Mater. **171-181**, 856 (1998).

[17] C. A. M. Mulder, A. J. van Duyneveldt, and J. A. Mydosh, Phys. Rev. B**23**, 1384 (1981).

[18] I. G. Deac, J. F. Mitchell, and P. Schiffer, Phys. Rev. B**63**, 172408 (2001).